

The **next generation** GBCA  
from Guerbet is here

Explore new possibilities >

Guerbet | 

© Guerbet 2024 GUOB220151-A

# AJNR

## **Cerebral aneurysms: evaluation with three-dimensional CT angiography.**

T Ogawa, T Okudera, K Noguchi, N Sasaki, A Inugami, K  
Uemura and N Yasui

*AJNR Am J Neuroradiol* 1996, 17 (3) 447-454  
<http://www.ajnr.org/content/17/3/447>

This information is current as  
of March 2, 2024.

# Cerebral Aneurysms: Evaluation with Three-dimensional CT Angiography

Toshihide Ogawa, Toshio Okudera, Kyo Noguchi, Nobuo Sasaki, Atsushi Inugami, Kazuo Uemura, and Nobuyuki Yasui

**PURPOSE:** To evaluate the usefulness of three-dimensional CT angiography (CTA), in which contrast material is used to create reformations of dynamic scans, in the diagnosis and the preoperative evaluation of cerebral aneurysms. **METHODS:** We used 3-D CTA to examine 65 patients with suspected or angiographically verified cerebral aneurysms. A blind study was performed to evaluate the diagnostic accuracy of 3-D CTA for cerebral aneurysms with the use of conventional angiography as the reference standard. **RESULTS:** In 50 patients, conventional angiography revealed 73 cerebral aneurysms ranging from 2 to 32 mm in maximum diameter. Three of the 73 cerebral aneurysms were located outside the imaging volume of 3-D CTA. The sensitivities of the two neuroradiologists for the remaining 70 aneurysms were 67% and 70%, respectively. Although 3-D CTA depicted cerebral aneurysms 5 mm or larger with good accuracy, it was less useful for the detection of smaller aneurysms. For the evaluation of giant aneurysms, this technique elucidated the relationships among the aneurysm, surrounding arteries, and neighboring bone structure. **CONCLUSION:** Three-dimensional CTA is useful for the diagnosis of cerebral aneurysms with diameters of 5 mm or more. This technique is especially useful in the preoperative evaluation of giant aneurysms.

**Index terms:** Aneurysm, cerebral; Aneurysm, computed tomography; Computed tomography, three-dimensional

*AJNR Am J Neuroradiol* 17:447-454, March 1996

Cerebral angiography is an essential technique in the diagnostic imaging and preoperative evaluation of cerebral aneurysms. However, it is invasive and carries a certain risk of complications (1, 2). Computed tomography (CT) with contrast medium has been used to confirm the presence of cerebral aneurysms (3-5). Schmid et al (4) reported the high accuracy of high-resolution CT in the direct diagnosis of cerebral aneurysms. Moreover, three-dimensional CT angiography (CTA), in which contrast material is used to create reformations of dynamic scans, has been successfully applied in the diagnosis of intracranial aneurysms

(6-8). Recent advances in helical CT have enabled neuroradiologists to evaluate cerebral aneurysms in a short time (9-11). Magnetic resonance (MR) angiography has also been reported to be useful in the diagnosis of cerebral aneurysms (12-17), but it is generally more time consuming than 3-D CTA, and it is extremely sensitive to motion artifacts. Furthermore, some aneurysms are not shown well by MR angiography because of turbulent or slow flow (13-16).

In this study, we examined 65 patients with 3-D CTA by using the procedures previously reported by Aoki et al (8), and we evaluated the usefulness of this technique in the diagnosis and the preoperative evaluation of cerebral aneurysms. Conventional angiography was used as the standard of reference.

## Materials and Methods

We reviewed retrospectively the findings in 65 patients (25 men and 40 women; age range, 41 to 79 years; mean age, 63 years), who had undergone conventional cerebral

---

Received July 1, 1993; accepted after revision September 25, 1995.

From the Department of Radiology and Nuclear Medicine (T.Og., T.Ok., K.N., N.S., A.I., K.U.) and Surgical Neurology (N.Y.), Research Institute of Brain and Blood Vessels—Akita, Japan.

Address reprint requests to Toshihide Ogawa, MD, Department of Radiology and Nuclear Medicine, Research Institute of Brain and Blood Vessels—Akita, 6-10, Senshu-kubota-machi, Akita City, 010, Akita, Japan.

*AJNR* 17:447-454, Mar 1996 0195-6108/96/1703-0447

© American Society of Neuroradiology

angiography before or after 3-D CTA. In 17 patients, the conventional angiography had been performed first and had shown an aneurysm; 3-D CTA had been performed within 7 days for comparison. The other 48 patients underwent 3-D CTA within 10 days before cerebral angiography. In 22 patients, 3-D CTA was performed because an aneurysm was suspected on the basis of findings on unenhanced CT scans; 17 patients were evaluated with 3-D CTA because of an aneurysm suspected on the basis of MR imaging; and in the 9 remaining patients, an aneurysm was suspected because of the clinical symptoms of oculomotor palsy.

Unenhanced CT scans (section thickness, 10 mm; section interval, 10 mm) were obtained parallel to the supraorbital-meatal line. After the selection of a starting point at the floor of the sella turcica, 100 mL of iopamidol (at the iodine concentration of 370 mg/mL) was injected intravenously at the rate of 1.0 mL/s by using a power injector via a 20-gauge polytef sheath needle inserted into the antecubital vein. The rapid sequential scanning (section thickness, 1.5 mm; section intervals, 1.5 mm) was started 45 seconds after the injection had been started. To include all of the circle of Willis, we obtained a total of 20 to 25 sections by scanning at 2 seconds per scan (intersection delay, 3.5 seconds). The time from the start of the injection until the end of the sequential scanning was about 2.8 minutes. The sequential scanning was performed under the following parameters: 120 kV; 120 mA; matrix,  $512 \times 512$ ; and field of view, 25 cm. Three-dimensional CT reformations were obtained by using the surface-rendering method on the computer-analyzing system for digital images. The thresholding technique used had a lower threshold of 80 to 90 Hounsfield units. Bone structures were not edited from the axial images. We obtained 8 to 15 images, each acquired at a different angle, by 3-D CTA. The total examination time, including 3-D reconstruction, was about 20 minutes.

Four-vessel cerebral angiography was performed by Seldinger's method via the femoral route. Anteroposterior, lateral, and oblique views were obtained with stereoscopic and magnification techniques. We calculated the sizes of the cerebral aneurysms after we had corrected for the magnification factor.

We performed a blind study to assess the diagnostic accuracy of the 3-D CTA findings in the identification of cerebral aneurysms. Two neuroradiologists independently reviewed and assessed the 3-D CT angiograms and their source images for the presence or absence of aneurysms. These neuroradiologists had no knowledge of the findings from conventional angiography. Seven 3-D CT images (anterosuperior, right and left anterosuperior oblique, superior, posterosuperior, right and left posterosuperior oblique views) were used for the blind study. After the blind study was complete, three neuroradiologists analyzed the 3-D CT angiograms along with the conventional angiograms with respect to the visibility of each aneurysm. A consensus of the three neuroradiologists determined whether the aneurysms identified on the conventional an-

giograms were shown on the 3-D CT angiograms. Their agreement was used for this analysis.

## Results

Seventy-three unruptured saccular aneurysms in 50 of the 65 patients were confirmed angiographically. In the other 15 patients, no aneurysms were shown on conventional angiograms. Thirty-five patients had 1 aneurysm, 9 had 2 aneurysms, 5 had 3 aneurysms, and 1 had 5 aneurysms. The aneurysms were located in the cavernous sinus ( $n = 2$ ), ophthalmic artery ( $n = 8$ ), posterior communicating artery ( $n = 10$ ), anterior choroidal artery ( $n = 2$ ), carotid bifurcation ( $n = 2$ ), horizontal portion of the anterior cerebral artery ( $n = 2$ ), pericallosal artery ( $n = 3$ ), anterior communicating artery ( $n = 10$ ), middle cerebral artery ( $n = 27$ ), vertebral artery ( $n = 2$ ), and basilar artery ( $n = 5$ ). The largest dimensions of the aneurysms ranged from 2 to 32 mm (mean  $\pm$  SD,  $9.5 \text{ mm} \pm 6.9$ ).

Sixty-one (84%) of the 73 aneurysms were identified on 3-D CTA. The remaining 12 aneurysms were not shown by 3-D CTA. Three aneurysms (1 in the pericallosal artery and 2 in the ophthalmic artery) were located outside the imaging volume; 4 aneurysms (all in the ophthalmic artery; size range, 2 to 5 mm) were not identified because they were mixed in the neighboring bone structures; and 5 aneurysms (1 each in the posterior communicating artery [3 mm], anterior cerebral artery [3 mm], and anterior communicating artery [3 mm], and 2 in the middle cerebral artery [2 mm and 3 mm]), were not seen because of their small size. Of the 61 aneurysms identified on 3-D CT angiograms, 14 (23%) were 4 mm or smaller.

Table 1 shows the results of the blind study of diagnostic accuracy. Because three aneurysms were located outside the imaging volume, we eliminated them from this analysis. In the detection of the remaining 70 aneurysms, the sensitivity was 70% for observer A and 67% for observer B. Of the 61 aneurysms that were confirmed on 3-D CTA by the three neuroradiologists, observer A detected 49 (80%) and observer B detected 47 (77%). Although the diagnostic accuracy of 3-D CTA in the identification of cerebral aneurysms depended mainly on the size of the aneurysm rather than the location, ophthalmic artery aneurysms were

TABLE 1: Diagnostic accuracy of 3-D CT angiograms in the blind study by two observers

Location	Size in Largest Dimension, mm					Total (%)
	2-4	5-7	8-10	11-13	≥14	
<b>Observer A</b>						
AcoA	2/4 (1)*	1/1	2/2	2/2	1/1	8/10 (80)
ACA	0/2 (1)*	1/2	...	...	...	1/4 (25)
MCA	2/10 (2)*	3/4	3/3	4/4	6/6	18/27 (67)
ICA	0/4 (3)*	2/5 (2)*	5/5	2/2	6/6	15/22 (68)
VA, BA	1/1	2/2	1/1	1/1	2/2	7/7 (100)
<b>Total</b>	<b>5/21</b>	<b>9/14</b>	<b>11/11</b>	<b>9/9</b>	<b>15/15</b>	<b>49/70</b>
Sensitivity	24%	64%	100%	100%	100%	70%
<b>Observer B</b>						
AcoA	1/4 (1)*	0/1	2/2	2/2	1/1	6/10 (60)
ACA	0/2 (1)*	1/2	...	...	...	1/4 (25)
MCA	3/10 (2)*	4/4	3/3	4/4	6/6	20/27 (74)
ICA	0/4 (3)*	1/5 (2)*	5/5	2/2	6/6	14/22 (64)
VA, BA	0/1	2/2	1/1	1/1	2/2	6/7 (86)
<b>Total</b>	<b>4/21</b>	<b>8/14</b>	<b>11/11</b>	<b>9/9</b>	<b>15/15</b>	<b>47/70</b>
Sensitivity	19%	57%	100%	100%	100%	67%

Note.—AcoA indicates anterior communicating artery; ACA, anterior cerebral artery (horizontal portion, and pericallosal artery); MCA, middle cerebral artery; ICA, internal carotid artery; VA, vertebral artery; and BA, basilar artery.

\* Number of aneurysms shown on conventional angiograms but not shown on 3-D CT angiograms, as determined by a consensus of three neuroradiologists.

generally difficult to detect because this artery is located adjacent to bone structures.

Eighteen of these 70 aneurysms were overlooked by both observers (Table 2). Nine of the 18 aneurysms were evaluated as not shown on the 3-D CT angiograms but shown on the conventional cerebral angiograms. Fifteen of the 18 aneurysms that were overlooked were 4 mm or smaller in diameter; the other three were ophthalmic artery aneurysms (5 or 6 mm) located adjacent to the anterior clinoid process. All aneurysms that were 5 mm or larger (except those three in the ophthalmic artery) were detected by either one or both of the observers.

TABLE 2: Cerebral aneurysms overlooked on 3-D CT angiograms by both observers in the blind study

Location of Aneurysm	Size in largest dimension, mm	Number
<b>Internal carotid artery</b>		
Anterior choroidal artery	4	1
Posterior communicating artery	3*, 3	2 (1*)
Ophthalmic artery	2*, 4*, 5*, 5*, 6	5 (4*)
Anterior communicating artery	3*, 3	2 (1*)
Anterior cerebral artery	3*, 4	2 (1*)
Middle cerebral artery	2*, 3*, 3, 3, 3, 4	6 (2*)
<b>Total</b>		<b>18 (9*)</b>

\* Aneurysms that were shown on conventional angiograms but not shown on 3-D CT angiograms, as determined by the consensus of three neuroradiologists.

When the criterion for a positive study was detection of at least one aneurysm, the sensitivity of 3-D CTA in the detection of aneurysms in 50 patients was 84% (42/50) for observer A and 82% (41/50) for observer B. The specificity was 100% for both observers. (However, this is a limited evaluation of specificity because only 15 subjects had no aneurysms.) The accuracy, therefore, was 88% (57/65) for observer A and 86% (56/65) for observer B. Each observer had two false-positive results, but both sets involved different aneurysms. The false-positive results were caused by the misinterpretation of the bending of an artery as an aneurysm. Although large venous structures such as the basal vein of Rosenthal were sometimes seen, these structures were not mistaken for aneurysms.

The 3-D CT angiograms afforded good visualization of the relationship of large aneurysms to the surrounding arteries and to the neighboring bone structures of the skull base (Figs 1-4). The ability to rotate the 3-D CT angiogram freely facilitated the understanding of these relationships. By manually eliminating the surrounding vessels and the adjacent bone structures that hinder the evaluation of the aneurysm on the digital-image computer-analysis system, we could evaluate these relationships in detail (Fig 3). Moreover, the inner surface could be observed by cutting through the aneurysm. This

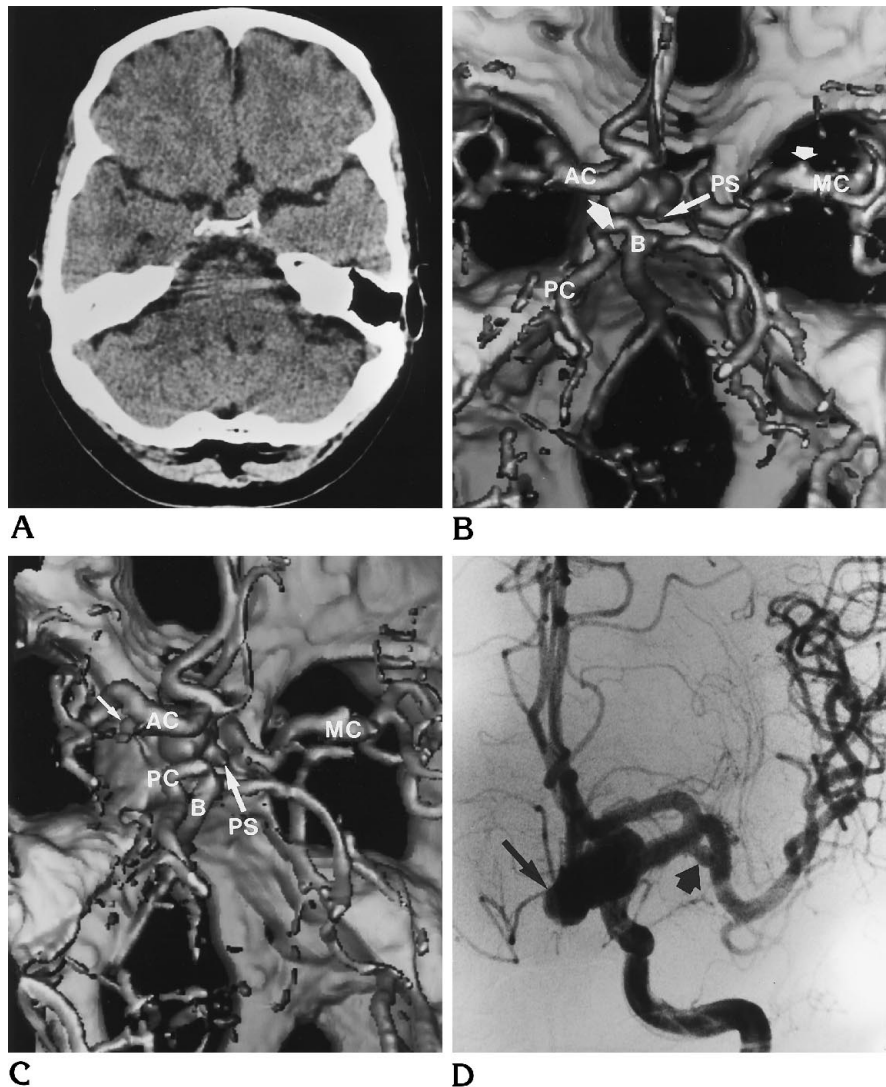
Fig 1. Woman 66 years old with aneurysms of the left internal carotid artery–posterior communicating artery (19 mm), left internal carotid artery–anterior choroidal artery (4 mm), and right middle cerebral artery (4 mm). AC indicates anterior cerebral artery; MC, middle cerebral artery; PC, posterior cerebral artery; B, basilar artery; and PS and *large thin arrow* in B and C, pituitary stalk.

A, Unenhanced CT scan depicts a round isodense mass in the suprasellar cistern.

B, Superior view (from above). Three-dimensional CT angiogram clearly shows a large aneurysm (*large wide arrow*) of the left internal carotid artery extending into the suprasellar cistern and sella turcica. The aneurysm of the right middle cerebral artery (*small wide arrow*) is also shown.

C, Posterosuperior and slightly lateral view. Three-dimensional CT angiogram shows a small aneurysm (*small thin arrow*) arising from the origin of the anterior choroidal artery.

D, Left internal carotid angiogram (frontal view) shows a large aneurysm of the internal carotid artery–posterior communicating artery (*long arrow*) and a small aneurysm of the internal carotid artery–anterior choroidal artery (*short arrow*).



information was especially useful for preoperative evaluation of aneurysms. However, we could not accurately evaluate intracavernous aneurysms because of the enhancement of the affected cavernous sinus.

## Discussion

Autopsy studies estimate that as many as 5% of the population may have aneurysms (18). The frequency of subarachnoid hemorrhage is approximately 11 per 100 000 persons in the United States (19). Approximately 28 000 people per year in North America sustain subarachnoid hemorrhage associated with aneurysmal rupture (20). However, according to the International Cooperative Study on the Timing of Aneurysm Surgery, only 58% of patients admitted to major neurosurgical units within 3

days of aneurysmal subarachnoid hemorrhages made a complete recovery, and 26% died (21). Therefore, we should consider the possibility of screening patients who are at high risk for intracranial aneurysms.

Cerebral angiography is still the reference standard for the diagnosis of cerebral aneurysms. However, this technique is invasive and carries a risk of complications (1, 2). The capacity to diagnose cerebral aneurysms reliably by noninvasive methods such as MR angiography and 3-D CTA could make possible the replacement of cerebral angiography by these noninvasive methods in the diagnostic imaging of cerebral aneurysms.

Yamamoto et al (3) reported that computed angiotomography was useful for the diagnosis of unruptured cerebral aneurysms. They found

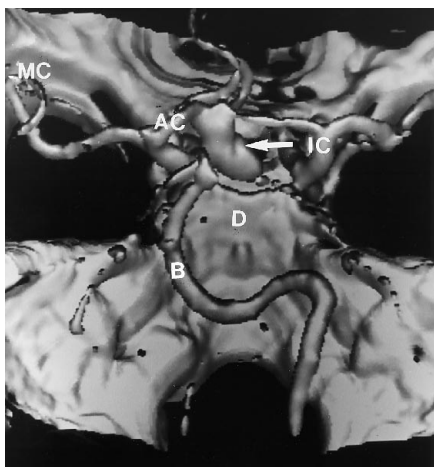


Fig 2. Woman 66 years old with a giant aneurysm (25 mm) at the anterior communicating artery. Three-dimensional CT angiogram (posterosuperior view) clearly shows a giant aneurysm (arrow) arising from the anterior communicating artery, extending into the sella turcica. *IC* indicates internal carotid artery; *AC*, anterior cerebral artery; *MC*, middle cerebral artery; *B*, basilar artery; and *D*, dorsum sellae.

that only aneurysms with diameters of more than 3 mm were shown by angiotomography. Schmid et al (4) reported that high-resolution CT with intravenous bolus injection of a contrast medium was helpful in the diagnosis of 74 (97%) of 76 cerebral aneurysms. Also, use of 3-D CTA has provided accurate evaluation of cerebral aneurysms. Aoki et al (8) initially reported that 3-D CT angiograms clearly showed all of 15 aneurysms that were 3 mm or larger in diameter. Moreover, the use of helical CT has shortened the scanning time needed (9–11). In the analysis of 30 angiographically verified aneurysms, Schwartz et al (11) reported that helical CT scans showed 26 (87%) of aneurysms that were 3 mm or larger in greatest dimension (mean size  $\pm$  SD, 9.47 mm  $\pm$  7.75).

In this study of a relatively large group of patients, we assessed the diagnostic accuracy of 3-D CTA in the identification of cerebral aneurysms. The sensitivity of the inspection of 3-D CT angiograms for cerebral aneurysms was 67% and 70% for two observers, respectively. The 3-D CT angiograms showed small (3 mm) as well as giant aneurysms, regardless of whether flow was turbulent or slow. However, small aneurysms, especially those located adjacent to bone structures (such as those arising from the origin of the ophthalmic artery) were not detected as readily as larger aneurysms. Moreover, as shown in Figures 1 through 4, a number of irregularities (or bumps) can be seen

on the arteries. The enhanced pituitary gland sometimes looks like an aneurysm. However, by viewing the 3-D CT angiograms from several different angles, we could usually distinguish cerebral aneurysms from incidental bumps and from the pituitary gland. If all such bumps were interpreted as aneurysms, the sensitivity for small aneurysms would increase but the rate of false-positive results would also increase.

On the other hand, MR angiography has developed rapidly, and several studies have evaluated the efficacy of MR angiography in depicting cerebral aneurysms (12–17). Ross et al (12) reported that MR angiography could define the circle of Willis well enough to allow the detection of intracranial aneurysms as small as 3 to 4 mm. Recently, Korogi et al (17) reported that MR angiography can depict intracranial aneurysms that are 5 mm or larger with good accuracy but is less useful for the identification of smaller aneurysms. Schwartz et al (11) compared 3-D CTA with MR angiography in the identification of cerebral aneurysms. They concluded that helical CT was comparable to standard MR angiography in showing aneurysms (11). All these researchers used the 3-D time-of-flight method to obtain the MR angiograms. Although this technique is suitable for the visualization of small aneurysms in a relatively short time, it has problems with showing large aneurysms and with distinguishing a patent lumen from a subacute thrombus containing methemoglobin (14–16). These disadvantages of the time-of-flight technique have been resolved by the application of the phase-contrast technique. However, the phase-contrast technique requires a relatively long examination time, despite the new phase-contrast pulse sequences that substantially shorten the examination time (14–16).

On the basis of our results, we think that the major advantage of 3-D CTA is its usefulness in the preoperative evaluation of large and giant aneurysms. In such cases, it is often difficult to show the neck of the aneurysm or the relationship between the aneurysm and the adjacent arteries on conventional cerebral angiography. Three-dimensional CTA clearly shows such relationships. Further, because we can see those aneurysms as well as the bone structures on 3-D CTA, it helps in making decisions about the most appropriate surgical approach. Napel et al (10) and Schwartz et al (11) reported a technique for obtaining CT angiograms by using

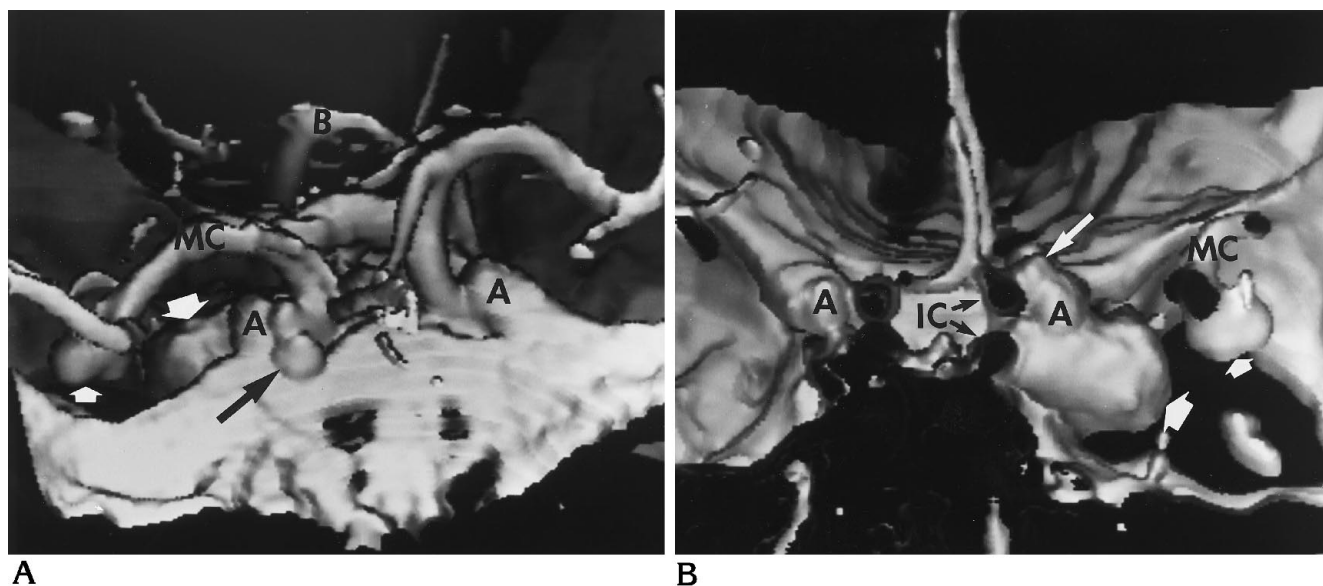


Fig 3. Man 60 years old with a giant aneurysm (26 mm) at the cavernous portion of the right internal carotid artery, and aneurysms of the right internal carotid artery–ophthalmic artery (12 mm), and right middle cerebral artery (10 mm). *IC* indicates internal carotid artery; *MC*, middle cerebral artery; *B*, basilar artery; and *A*, anterior clinoid process.

*A*, Three-dimensional CT angiogram (superior and right anterior oblique view) shows an internal carotid artery–ophthalmic artery aneurysm (*long black arrow*), a giant cavernous aneurysm of the right internal carotid artery (*large white arrow*), and a middle cerebral artery bifurcation aneurysm (*small white arrow*). The relationship between the right internal carotid artery–ophthalmic artery aneurysm and the right anterior clinoid process is clearly shown.

*B*, After manual elimination of the posterior half of the skull and vascular structures, 3-D CT angiogram (posterior view; the right side of the patient is on the reader's right) clearly shows the relationships among the right internal carotid artery–ophthalmic artery aneurysm (*long thin arrow*), the giant cavernous aneurysm of the right internal carotid artery (*large wide arrow*), and the right anterior clinoid process. Right middle cerebral artery aneurysm (*small wide arrow*) is also clearly seen.

*C*, The right internal carotid artery–ophthalmic artery aneurysm is not distinguished from the giant cavernous aneurysm of the internal carotid artery (*long arrow*) on the frontal-view angiogram of the right common carotid artery. The right middle cerebral artery aneurysm (*short arrow*) is clearly seen.



helical CT and the maximum-intensity projection method (10, 11). After the bone structure at the skull base is excluded from the axial images, the maximum-intensity projection method is useful for the evaluation of small aneurysms adjacent to bone structures. However, because this technique suppresses bone structure, the physician loses the benefit of observing simultaneously the cerebral aneurysms and the bone structure, as can be done with 3-D CTA. Therefore, we think that the combined use of the maximum-intensity projection method and our method is an appropriate policy for the evaluation of cerebral aneurysms.

Compared with MR angiography, 3-D CTA has the disadvantages of radiation exposure and the need for iodinated contrast material. The radiation dose to the skin surface in the 3-D CTA method we used is 2.4 to 18.5 mSv, according to the report by Sasaki et al (22). This is lower than the dose received during routine head CT scanning and is acceptable for a clinical examination. Another problem in our study was that 3 of the 73 aneurysms were located outside the imaging volume, but this problem has recently been solved by the use of helical CT, by which a large imaging volume can be covered in a shorter time (11).

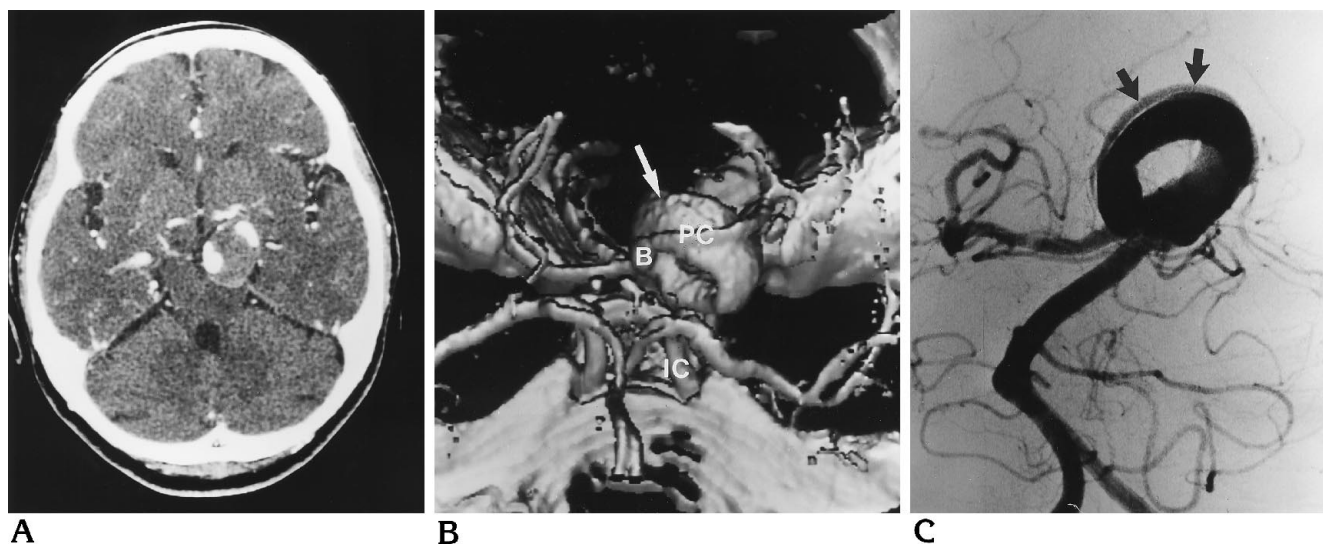


Fig 4. Woman 56 years old with a large aneurysm of the basilar artery (22 mm).

A, Source image of 3-D CT angiogram shows a round aneurysm compressing the upper portion of the pons. This large aneurysm is composed of the two parts of a patent lumen and an organized thrombus.

B, Three-dimensional CT angiogram (anterosuperior view) clearly shows the large aneurysm with a doughnut shape (arrow) arising from the basilar artery. The left posterior cerebral artery is elevated by the aneurysm. From this view, it is easy to understand the relationships among the aneurysm, the surrounding arteries, and the skull base. IC indicates internal carotid artery; PC, posterior cerebral artery; and B, basilar artery.

C, Right vertebral angiogram (frontal view) reveals the large basilar artery aneurysm as a doughnut-shaped structure. The left posterior cerebral artery (arrows) is elevated by the aneurysm.

In our study, most cerebral aneurysms larger than 5 mm in diameter were shown well. Yamamoto et al (3) reported that an isodense round cisternal defect and a calcification or high-density mass in the basal cisterns shown on unenhanced CT scans were important findings that suggest unruptured aneurysms larger than 7 mm in diameter. Therefore, if we intend to confirm the presence of an aneurysm by using contrast-enhanced CT, 3-D CTA is the most suitable method for the evaluation of unruptured aneurysms suspected on the basis of unenhanced CT findings. However, if MR angiography is as easily available as CT, the presence of an aneurysm suspected on the basis of unenhanced CT scans may be confirmed by MR angiography also. As the detection rate of aneurysms for 3-D CTA seems to be similar to that for MR angiography in both our study and previous studies (11, 17), it seems that the method can be selected on the basis of the availability of each technique and the patient's condition.

Our results indicate that 3-D CTA is not an effective tool for searching for small aneurysms. However, because 3-D CTA can show simultaneously cerebral aneurysms and bone struc-

tures, it is helpful for the preoperative evaluation of cerebral aneurysms.

In conclusion, despite some disadvantages associated with the use of contrast material, 3-D CTA is useful for the diagnosis of cerebral aneurysms 5 mm or larger in diameter and is especially powerful in the preoperative evaluation of giant aneurysms.

## References

1. Earnest F IV, Forbes G, Sandok BA, et al. Complications of cerebral angiography: prospective assessment of risk. *AJNR Am J Neuroradiol* 1983;4:1191-1197
2. Hankey GJ, Warlow CP, Sellar RJ. Cerebral angiographic risk in mild cerebrovascular disease. *Stroke* 1990;21:209-222
3. Yamamoto Y, Asari S, Sunami N, Kunishio K, Fukui K, Sadamoto K. Computed angiogram of unruptured cerebral aneurysms. *J Comput Assist Tomogr* 1986;10:21-27
4. Schmid UD, Steiger HJ, Huber P. Accuracy of high resolution computed tomography in direct diagnosis of cerebral aneurysms. *Neuroradiology* 1987;29:152-159
5. Teasdale E, Statham P, Straiton J, Macpherson P. Non-invasive radiological investigation for oculomotor palsy. *J Neurol Neurosurg Psychiatry* 1990;53:549-553
6. Gillespie JE, Adams JE, Isherwood I. Three-dimensional computed tomographic reformations of sellar and para-sellar lesions. *Neuroradiology* 1987;29:30-35



7. Gholkar A, Isherwood I. Three-dimensional computed tomographic reformations of intracranial vascular lesions. *Br J Radiol* 1988;61:258-261
8. Aoki S, Sasaki Y, Machida T, Ohkubo T, Minami M, Sasaki Y. Cerebral aneurysm: detection and delineation using 3-D-CT angiography. *AJNR Am J Neuroradiol* 1992;13:1115-1120
9. Katada K, Anno H, Koga S, Ikuta K, Ida Y, Yamagishi I. Three-dimensional angiography with helical scanning CT. *Radiology* 1990;177(suppl):364
10. Napel S, Marks MP, Rubin GD, et al. CT angiography with spiral CT and maximum intensity projection. *Radiology* 1992;185:607-610
11. Schwartz RB, Tice HM, Hooten SM, Hsu L, Stieg PE. Evaluation of cerebral aneurysms with helical CT: correlation with conventional angiography and MR angiography. *Radiology* 1994;192:717-722
12. Ross JS, Masaryk TJ, Modic MT, Ruggieri PM, Haacke EM, Selman WR. Intracranial aneurysms: evaluation by MR angiography. *AJNR Am J Neuroradiol* 1990;11:449-456
13. Masaryk TJ, Modic MT, Ross JS, et al. Intracranial circulation: preliminary clinical results with three-dimensional (volume) MR angiography. *Radiology* 1989;171:793-799
14. Huston J III, Rufenacht DA, Ehman RL, Wiebers DO. Intracranial aneurysms and vascular malformations: comparison of time-of-flight and phase-contrast MR angiography. *Radiology* 1991;181:721-730
15. Huston J III, Ehman RL. Comparison of time-of-flight and phase-contrast MR neuroangiographic techniques. *RadioGraphics* 1993;13:5-19
16. Pernicone JR. Intracranial aneurysm. In: Patterson AS, ed. *Magnetic Resonance Angiography*. St Louis, Mo: Mosby, 1993:405-431
17. Korogi Y, Takahashi M, Mabuchi N, et al. Intracranial aneurysms: diagnostic accuracy of three-dimensional, Fourier transform, time-of-flight MR angiography. *Radiology* 1994;193:181-186
18. Mohr JP, Kistler JP, Fink ME. Intracranial aneurysms. In: Barnett HJM, Stein BM, Mohr JP, Yatsu FM, eds. *Stroke: Pathophysiology, Diagnosis, and Management*. New York, NY: Churchill Livingstone, 1986:617-643
19. Phillips LH, Whisnant JP, O'Fallon M, Sundt TM. The unchanging pattern of subarachnoid hemorrhage in a community. *Neurology* 1980;30:1034-1040
20. Davis JM, Hesselink JR. Vascular lesions: intracerebral hemorrhage. In: Taveras JM, Ferrucci JT, eds. *Radiology: Diagnosis—Imaging—Intervention*. Philadelphia, Pa: Lippincott, 1988:1-15
21. Kassell NF, Torner JC, Haley EC, et al. The International Cooperative Study on the Timing of Aneurysm Surgery, part 1: overall management results. *J Neurosurg* 1990;73:18-36
22. Sasaki N, Ogawa T, Kan M, et al. Evaluation of appropriate imaging parameters for 3D-CT angiography for the diagnosis of cerebral aneurysm. *J Jpn Assoc Radio Technol* 1993;40:700-704